The Canadian Mineralogist
Vol. 37, pp. 603-617 (1999)

MINERALOGY OF THE ARCHEAN BARITE DEPOSIT OF GHATTIHOSAHALLI, KARNATAKA, INDIA

TADASORE C. DEVARAJU

Department of Studies in Geology, Karnatak University, Dharwad 580 003, India

MICHAEL M. RAITH[1] AND BEATE SPIERING

Mineralogisch-Petrologisches Institut, Universität Bonn, Poppelsdorfer Schloß, D-53115 Bonn, Germany

ABSTRACT

The mineralogy of the mid-Archean barite deposit in the Ghattihosahalli supracrustal belt in central Karnataka, India, has been comprehensively investigated. The deposit occurs as thin seams closely associated with chromiferous quartzites located in the upper part of a stratigraphic sequence consisting of mafic and ultramafic rocks in the lower portion and predominantly siliceous to argillaceous sediments in the middle. The belt has undergone medium-pressure amphibolite-facies metamorphism. The predominant variety of barite is coarse grained and contains only minor amounts of quartz, pyrite and scarce graphite. In contrast, the fine-grained impure barite, which constitutes a smaller proportion of the deposit, contains a spectrum of Ba–Cr minerals. These include (1) barian-chromian mica showing a significant solid-solution toward the barian end-member $Ba(Mg,Fe^{2+})Al[AlSi_3O_{10}](OH)_2$, (2) K,Ba-feldspar covering the entire solid-solution from K-feldspar to celsian, with a compositional gap between $Or_{62}Cn_{30}Ab_{08}$ and $Or_{88}Cn_{08}Ab_{04}$, (3) chromian dravite (3–19 wt.% Cr_2O_3), (4) epidote containing up to 80 mol.% of the $Cr^{3+}Al_2$ end-member, (5) uvarovitic garnet ($Uva_{61}Grs_{34}$ – $Uva_{41}Grs_{52}$), (6) rutile and titanite with up to 2.8 and 1.6 wt.% Cr_2O_3, respectively. Mineral compositions vary considerably from one seam to the other; within the limits of individual samples, the variations are largely controlled by the bulk composition of the rock. The stratiform nature and lithological association, together with the mineralogical and chemical characteristics, suggest a mode of formation through submarine volcanic exhalation and precipitation, with a minor interplay of clastic sedimentation.

Keywords: barite deposit, Archean, K,Ba-feldspar, Ba,Cr-bearing minerals, Ghattihosahalli, India.

SOMMAIRE

La minéralogie d'un gisement de barite d'âge archéen moyen dans la ceinture de roches supracrustales de Ghattihosahalli, dans le centre de l'état de Karnataka, en Inde, a été étudié de façon compréhensive. Le gisement se présente sous forme de mince couches étroitement associées avec des quartzites chromifères situées dans la partie supérieure de la séquence stratigraphique comprenant des roches mafiques et ultramafiques dans la partie inférieure et surtout des roches siliceuses et argileuses dans la partie du milieu. Cette ceinture a subi les effets d'une recristallisation à pression moyenne dans le faciès amphibolite. La variété prédominante de barite, à grains grossiers, ne contient que des quantités infimes de quartz, pyrite et graphite. En revanche, la barite à granulométrie fine, qui constitue une partie moins importante du gisement, contient une variété de minéraux de Ba–Cr, y inclus (1) mica riche en Ba et Cr, montrant une solution solide importante vers le pôle $Ba(Mg,Fe^{2+})Al[AlSi_3O_{10}](OH)_2$, (2) feldspath potassique et barifère représentant toute la série entre feldspath potassique et celsian, sauf une lacune entre $Or_{62}Cn_{30}Ab_{08}$ et $Or_{88}Cn_{08}Ab_{04}$, (3) dravite chromifère (3–19% Cr_2O_3, poids), (4) épidote contenant jusqu'à 80% (base molaire) du pôle $Cr^{3+}Al_2$, (5) grenat uvarovitique ($Uva_{61}Grs_{34}$ – $Uva_{41}Grs_{52}$), (6) rutile et titanite ayant jusqu'à 2.8 et 1.6% de Cr_2O_3, respectivement. La composition des minéraux varie considérablement d'une couche à l'autre; les variations semblent dépendre largement de la composition globale des roches. La nature stratiforme et l'association lithologique, de même que les caractéristiques des associations de minéraux et des compositions, font penser qu'il s'agit d'un gisement volcanogénique formé par exhalations sous-marines, avec une légère contribution due à la sédimentation clastique.

(Traduit par la Rédaction)

Mots-clés: gisement archéen de barite, feldspath K,Ba, minéraux Ba–Cr, Ghattihosahalli, Inde.

[1] *E-mail address*: m.raith@uni-bonn.de

Introduction

The occurrence of barite seams interstratified with quartzite of the Ghattihosahalli schist belt was first reported by Radhakrishna & Sreenivasaiya (1974). Subsequently, besides exploration to assess the size and quality of the deposit by the State Department of Mines and Geology (Annaiya & Srinivasaiah 1976), the barite and the associated lithologies have been examined by Viswanatha *et al.* (1977), Naqvi (1978), Chadwick *et al.* (1978, 1981, 1985), Devaraju & Anantha Murthy (1978, 1979), Narayana & Naqvi (1980), Seshadri *et al.* (1981), Raase *et al.* (1983), Hoering (1989) and Devaraju & Raith (1990). The present study supplements the available information with comprehensive analytical data for the various minerals present in the deposit. Also, we discuss the genesis of the deposit in the light of the new data obtained.

Occurrence

The Ghattihosahalli schist belt, in which the barite deposit occurs, is regarded as the equivalent of greenstone rocks of the Archean (>3.0 Ga) Sargur Group. It is a narrow, 25-km-long belt lying just west of the main Chitradurga schist belt (Karnataka). It occurs partly as an enclave within tonalitic gneisses (3.0–3.1 Ga: Taylor *et al.* 1984) and partly in juxtaposition with the younger Dharwar supracrustal rocks of the Chitradurga belt (Fig. 1). The Ghattihosahalli belt consists of metamorphosed ultramafic to mafic igneous rocks (serpentinite, locally showing a spinifex texture, talc–tremolite schist and amphibolites) in the lower section, and a sequence of siliceous metasedimentary units in the upper section (Fig. 2). The lithologies of the belt display an older fabric associated with medium-grade mineral assemblages (*e.g.*, staurolite + garnet + kyanite + musco-

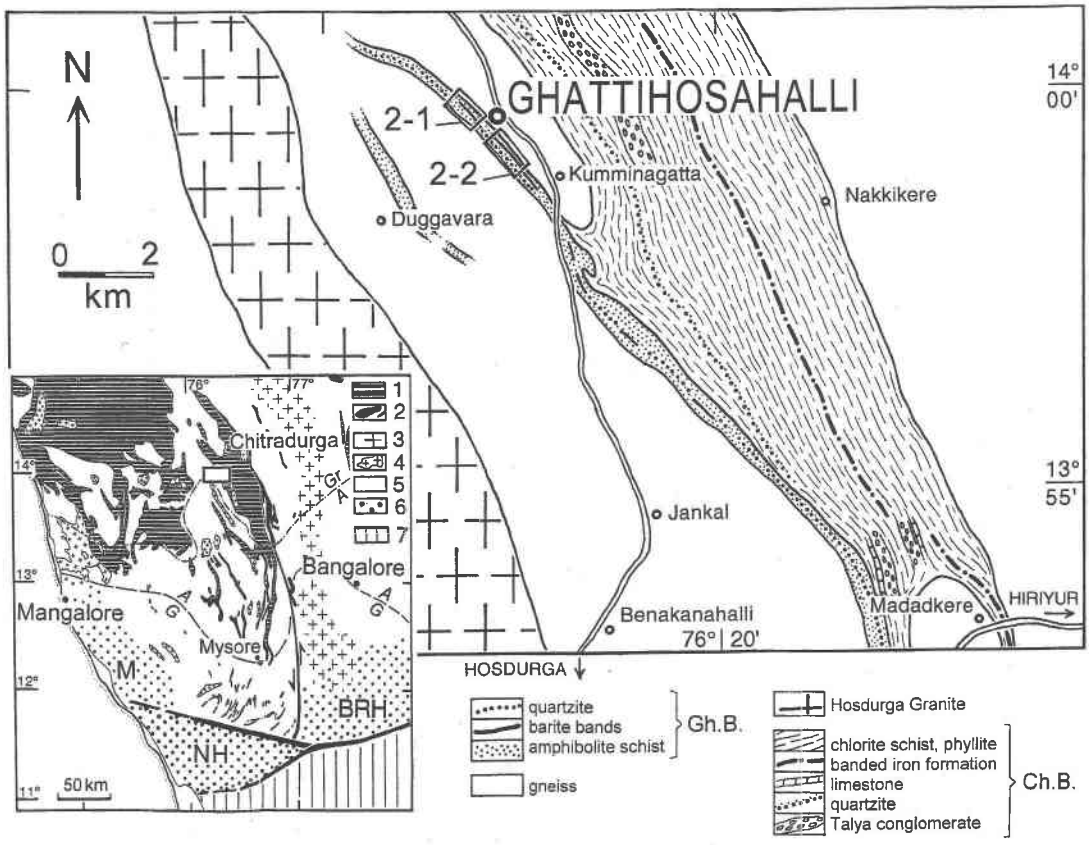

FIG. 1. Simplified geological map showing the Ghattihosahalli schist belt (Gh.B.) and the barite occurrences. The inset map illustrates the geological framework of the Archean Karnataka craton (after Raase *et al.* 1983). Legend: 1 Dharwar Supergroup schist belts, 2 greenstone belts of the Sargur Group, 3 late Archean Closepet granitic rocks, 4 granitic rocks, 5 polyphase mid-Archean tonalitic–trondhjemitic gneisses and plutonic rocks, 6 granulite terranes of the Mercara region (M), the Nilgiri (NH) and Biligirirangan Hill (BRH) ranges, 7 gneiss terrane south of the Bhavani shear zone affected by strong Pan-African reworking. Gr/A and A/G: boundaries separating the late Archean greenschist-, amphibolite- and granulite-facies domains within the Karnataka Craton. Ch.B: Chitradurga belt. Box indicates the position of the study area.

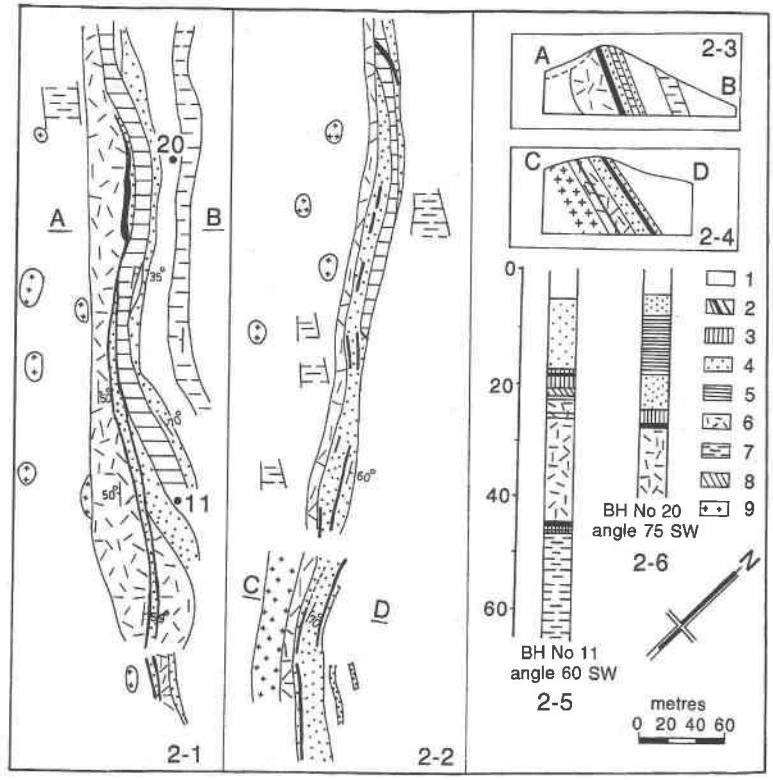

FIG. 2. Geological maps of the northern (2–1) and southern (2–2) domains of the Ghattihosahalli schist belt, containing the largest known seams of barite in the area (see Fig. 1). Figures 2–3 and 2–4 show sections across the northern and southern domains. Figures 2–5 and 2–6 provide drill-core logs penetrating the schist belt in the northern domain at points 11 and 20. Legend: 1 soil cover, 2 barite seams, 3 chromian muscovite quartzite, 4 gray quartzite, 5 quartz–white mica schist, 6 tremolite–actinolite schist, 7 hornblende schist, 8 mica schist, 9 granite.

vite in impure quartzites) and a younger fabric with development of low-grade assemblages (*e.g.*, chloritoid + chlorite + kyanite + muscovite in impure quartzites) related to late Archean deformation and metamorphism of the Dharwar supracrustal rocks (Chadwick *et al.* 1985).

Barite occurs as conformable but discontinuous thin bands and lenses in a narrow (5 to 20 m) zone within the quartzites, close to the underlying metabasic and meta-ultrabasic units (Fig. 2). With the single exception of the largest body, which is 1.25 m wide and 120 m long, all other barite layers are only several centimeters to half a meter in thickness and rarely persist along strike for more than 50 m. It is a stratiform deposit displaying relatively sharp contacts with the enclosing quartzites. There are no discordant veins or tongues of barite. Although quartzite varies widely in purity and texture, it can be broadly separated into two main types: (1) the more abundant gray-white massive quartzite with variable proportions of kyanite, staurolite, garnet, chlorite, chloritoid, grunerite, white mica and, locally, detrital chromite, tourmaline and zircon, with bedding defined by concentrations of metamorphic minerals into bands a few mm thick (Chadwick *et al.* 1985), and (2) the greenish chromiferous quartzite containing chromian muscovite and locally, bluish kyanite. The barite is largely confined to the chromiferous quartzite horizon.

PETROGRAPHY

Barite is fine- to coarse-grained and white to light gray in color. The coarse-grained variety usually contains the smallest proportion of included quartz. The only other important mineral present is pyrite, which occurs as disseminated, almost equant euhedral grains, generally arranged parallel to the stratification. This variety shows typical interlocking textures and gener-

ally bears little evidence of strain. The fine-grained barite commonly contains thin (<2–3 mm) bands of quartzite, less commonly disconnected bands and strings enriched in a variety of silicate and sulfide minerals, and bears evidence of shearing. A pronounced lineation parallel to the regional northwesterly structural grain of the schist belt is persistent irrespective of variations in grain size in the individual lenses of barite. In thin section, the fine-grained barite displays granoblastic textures with interlocking to polygonal grain-boundaries, locally with coarse grains, as compared with the fine-grained equigranular interlocking sutured texture of the host quartzite.

Mineralogy

Mineralogically, the barite layers of Ghattihosahalli contain 60–90 vol.% barite, and the remainder is mostly quartz. Pyrite is a ubiquitous minor constituent. The other minerals, namely barian–chromian mica, K,Ba-feldspar, tremolite, tourmaline, epidote and garnet, are important only in the more siliceous and fine-grained portions. Plagioclase, titanite, rutile and graphite are rare.

The minerals have been analyzed with a Cameca Camebax electron microprobe at the University of Bonn. The operating conditions were: accelerating voltage 15 kV, beam current 15 nA, spot size 1–2 μm, counting time 20 s. Both natural and synthetic mineral standards were used. Data processing was performed with the PAP correction procedure (Pouchou & Pichoir 1984).

Although quite fresh both in hand specimen and in thin sections, *barite* is seldom devoid of trains of gray to brown dusty inclusions, which occupy planes of weakness. Globular and ovoid aqueous fluid inclusions are common. Polysynthetic glide twinning on (110) is not unusual. Wavy extinction is limited to the sheared portions. For further details concerning optical and X-ray-diffraction characteristics, refer to Devaraju & Anantha Murthy (1979). Chemically, the barite of Ghattihosahalli is essentially pure $BaSO_4$. Sr contents are below the limit of detection.

Pyrite is widely distributed both in the coarse- and fine-grained layers of barite, where it is usually concentrated in thin discontinuous bands and stringers, and tends to occur as subhedral to euhedral grains measuring up to 3 mm in across. The pyrite contains 0.1–1.5 wt.% Ni and 0.1–3 wt.% Co (Table 1). Whereas Ni shows a well-defined negative correlation with iron (Fig. 3A), such correlation is not displayed by Co (Fig. 3B). Commonly, pyrite is altered to goethite along the grain boundaries. There is a positive correlation in the Co/Ni value between the two phases (Fig. 3C). Si, Al, Cu and Zn are other constituents recorded in the composition of goethite (Table 2).

K,Ba-feldspar occurs in typically ovoid porphyroblasts as well as interstitial euhedral grains, and may account for up to 30 vol.% in the samples of fine-grained barite. In thin section, the mineral shows up distinctly owing to the presence of a dark rim of iron oxide along grain boundaries and the distinctly lower relief compared to barite. The K,Ba-feldspar covers the compositional range from $Or_{90}Cn_{06}Ab_{04}$ to $Or_{03}Cn_{95}Ab_{02}$, *i.e.*, from barian orthoclase to celsian, with a gap in solid solution between $Or_{62}Cn_{30}Ab_{08}$ and $Or_{88}Cn_{08}Ab_{04}$ (Table 3, Fig. 4A). A similar compositional gap has been observed in several low- to medium-grade terranes (*e.g.*, Chabu & Boulègue 1992, Pan & Fleet 1991) and presumably represents a miscibility gap along the Or–Cn binary join. The albite component increases steadily from 2 mol.% in the celsian end-member to 12 mol.% in the intermediate part of the solid solution. Most of the samples studied contain unzoned grains of K,Ba-

TABLE 1. REPRESENTATIVE COMPOSITIONS OF PYRITE IN BARITE SEAMS FROM GHATTIHOSAHALLI

Sample	36A			140		33A				135			141		
Analysis	#21	#24	#27	#61	#62	#81	#46	#47	#48	#32	#33	#34	#38	#39	#41
Fe wt.%	45.78	45.56	44.89	45.72	45.94	45.86	44.63	44.72	45.07	45.04	45.13	46.08	45.97	45.88	46.12
Co	0.39	0.47	0.45	0.03	0.09	0.26	0.13	0.16	0.15	0.46	0.37	0.26	0.36	0.37	0.34
Ni	0.65	0.86	0.69	0.27	0.27	0.79	1.18	0.85	1.21	1.41	1.03	0.84	0.64	0.75	0.26
Cu	0.01	0.11	0.00	0.03	0.13	0.04	0.00	0.04	0.01	0.05	0.02	0.06	0.00	0.07	0.02
Zn	0.00	0.06	0.09	0.05	0.00	0.00	0.10	0.08	0.02	0.11	0.03	0.00	0.04	0.02	0.00
S	53.48	53.30	54.23	54.42	54.08	54.22	54.14	54.24	54.31	53.72	53.76	53.30	53.45	53.25	53.48
Total	100.31	100.36	100.35	100.52	100.51	101.17	100.18	100.09	100.77	100.79	100.34	100.54	100.46	100.34	100.22
Atomic proportions															
Fe apfu	0.978	0.970	0.974	0.992	0.990	0.978	0.971	0.976	0.971	0.959	0.970	0.976	0.979	0.975	0.987
Co	0.008	0.010	0.009	0.001	0.002	0.005	0.003	0.003	0.003	0.009	0.008	0.005	0.007	0.008	0.007
Ni	0.013	0.018	0.014	0.006	0.006	0.016	0.025	0.018	0.025	0.029	0.021	0.017	0.013	0.015	0.005
Cu	0.000	0.002	0.000	0.001	0.003	0.001	0.000	0.001	0.000	0.001	0.000	0.001	0.000	0.001	0.000
Zn	0.000	0.001	0.002	0.001	0.000	0.000	0.002	0.002	0.000	0.002	0.001	0.000	0.001	0.000	0.000
Co/Ni	0.598	0.545	0.650	0.111	0.332	0.328	0.110	0.188	0.124	0.325	0.358	0.309	0.561	0.492	1.304

TABLE 2. REPRESENTATIVE COMPOSITIONS OF GOETHITE IN BARITE SEAMS FROM GHATTIHOSAHALLI

Sample	36A			135		140	137			141	
Analysis	#25	#26	#22	#30	#31	#63	#24	#26	#27	#35	#40
SiO_2 wt.%	4.30	3.37	4.81	3.32	5.06	2.20	3.34	3.04	5.31	2.40	3.97
TiO_2	0.04	0.00	0.03	0.00	0.00	0.02	0.03	0.00	0.00	0.23	0.00
Al_2O_3	0.62	0.05	0.02	0.03	0.00	0.08	1.28	0.16	1.91	0.54	0.10
Cr_2O_3	0.01	0.00	0.03	0.00	0.00	0.00	0.00	0.08	0.00	0.00	0.00
V_2O_3	0.00	0.00	0.00	0.00	0.02	0.00	0.04	0.03	0.07	0.00	0.00
Fe_2O_3	78.53	79.33	79.13	80.02	85.68	83.06	81.01	85.53	80.20	73.25	81.39
MgO	0.09	0.04	0.04	0.00	0.00	0.03	0.12	0.04	0.08	0.03	0.03
CoO	0.37	0.13	0.55	0.68	0.09	0.02	0.00	0.54	0.00	0.41	0.29
NiO	0.84	0.79	1.05	1.04	0.34	0.35	0.20	1.77	0.03	0.72	0.52
CuO	1.17	1.63	0.65	1.19	0.69	0.03	0.32	0.00	0.32	0.43	0.83
ZnO	0.73	0.32	0.32	0.16	0.00	0.00	1.01	0.21	0.84	0.06	0.07
S	0.20	0.77	0.03	0.25	0.17	0.02	0.03	0.05	0.03	1.39	0.91
Total	86.92	86.41	86.65	86.70	92.05	85.81	87.38	91.45	88.78	79.44	88.09
Atomic proportions											
Fe^{3+} apfu	0.961	0.964	0.967	0.962	0.987	0.995	0.981	0.970	0.986	0.977	0.979
Co	0.005	0.002	0.007	0.009	0.001	0.000	0.000	0.007	0.000	0.006	0.004
Ni	0.011	0.010	0.014	0.013	0.004	0.004	0.003	0.021	0.000	0.010	0.007
Cu	0.014	0.020	0.008	0.014	0.008	0.000	0.004	0.000	0.004	0.006	0.010
Zn	0.009	0.004	0.004	0.002	0.000	0.000	0.012	0.002	0.010	0.001	0.001
Co/Ni	0.444	0.158	0.525	0.657	0.258	0.057	0.000	0.306	0.000	0.567	0.561

feldspar of distinct compositions that presumably were controlled by the bulk chemistry. A few samples contain grains of K,Ba-feldspar that exhibit discontinuous concentric patterns of zoning. For example, in sample 138, celsian cores (Cn_{95-90}) are overgrown by a broad inner rim ranging from Cn_{70} to Cn_{50}, a narrow outer rim with Cn_{40}, and finally by incomplete veneers of either K-feldspar or albite (Fig. 4B, Table 3).

Plagioclase occurs rarely in the fine-grained siliceous portion as untwinned to faintly twinned small but discrete laths or as a thin overgrowth around K,Ba-feldspar. It is virtually pure albite (Table 3).

Ba–Cr mica is limited mainly to the borders of barite bands with interstratified chromiferous quartzite. The compositional variation in the micas is essentially controlled by the coupled substitutions $^{VI}(Mg, Fe^{2+}) + {}^{IV}Si \rightleftharpoons {}^{VI}Al + {}^{IV}Al$ and $^{XII}(K,Na) + {}^{IV}Si \rightleftharpoons {}^{XII}Ba + {}^{IV}Al$, which in combination lead to the barian end-member $[Ba(Mg,Fe^{2+})Al[AlSi_3O_{10}](OH)_2]$, and by the partial replacement of Al by Cr in the octahedral sites, leading toward its chromian analogue (Figs. 5A, B, Table 4). There is a continuous compositional variation from Ba-poor chromian muscovite in the interstratified chromiferous quartzite to Ba-rich chromian mica attaining up to 35 mol.% of the barian end-member component in the barite layers (Fig. 5A), reflecting a control by the bulk composition. No correlation exists between Cr and Ba in the mica (Fig. 5B). These observations may be compared with the data obtained for mica from other chromiferous quartzites of comparable Sargur-type rocks that are not associated with barite; the chromian mica there is devoid of Ba, and its composition is controlled by the substitutions $^{VI}(Mg, Fe^{2+}) + {}^{IV}Si \rightleftharpoons {}^{VI}Al + {}^{IV}Al$ and $^{VI}Al \rightleftharpoons {}^{VI}Cr$ (Raase *et al.* 1983) (Figs. 5A, B). Furthermore, the interlayer occupancy of K, Ba, and Na in the micas of the barite layers and chromiferous quartzites, shown in Figure 5C, reveals essentially a constant level of the paragonite component (10–20 mol.%) over the recorded K–Ba solid-solution range (Fig. 5C). The observed compositional field possibly defines the miscibility limit in the muscovite – paragonite – barian mica system (*cf.* Tracy 1991).

Amphibole is restricted to some of the fine-grained samples. It is present in relatively coarse and very elongate crystals. Compositions range from pure tremolite to mangnesiohornblende, with actinolite compositions being most common (Table 5, Fig. 6). Chromium contents commonly are very low (<0.03 atoms per formula unit, *apfu*). The zoned crystals in samples 138 and 137b show a colorless tremolitic core that is overgrown by a rim of bluish green actinolite. The pattern of zonation indicates growth during a metamorphic episode progressing from greenschist- to amphibolite-facies conditions.

Tourmaline occurs sporadically as small subhedral to euhedral prismatic grains in the bands of fine-grained barite. Chemically, it is close to dravite, with minor variation toward uvite and elbaite (Fig. 7A). A striking feature is the high Cr content, responsible for the conspicuous green to emerald green color in thin section.

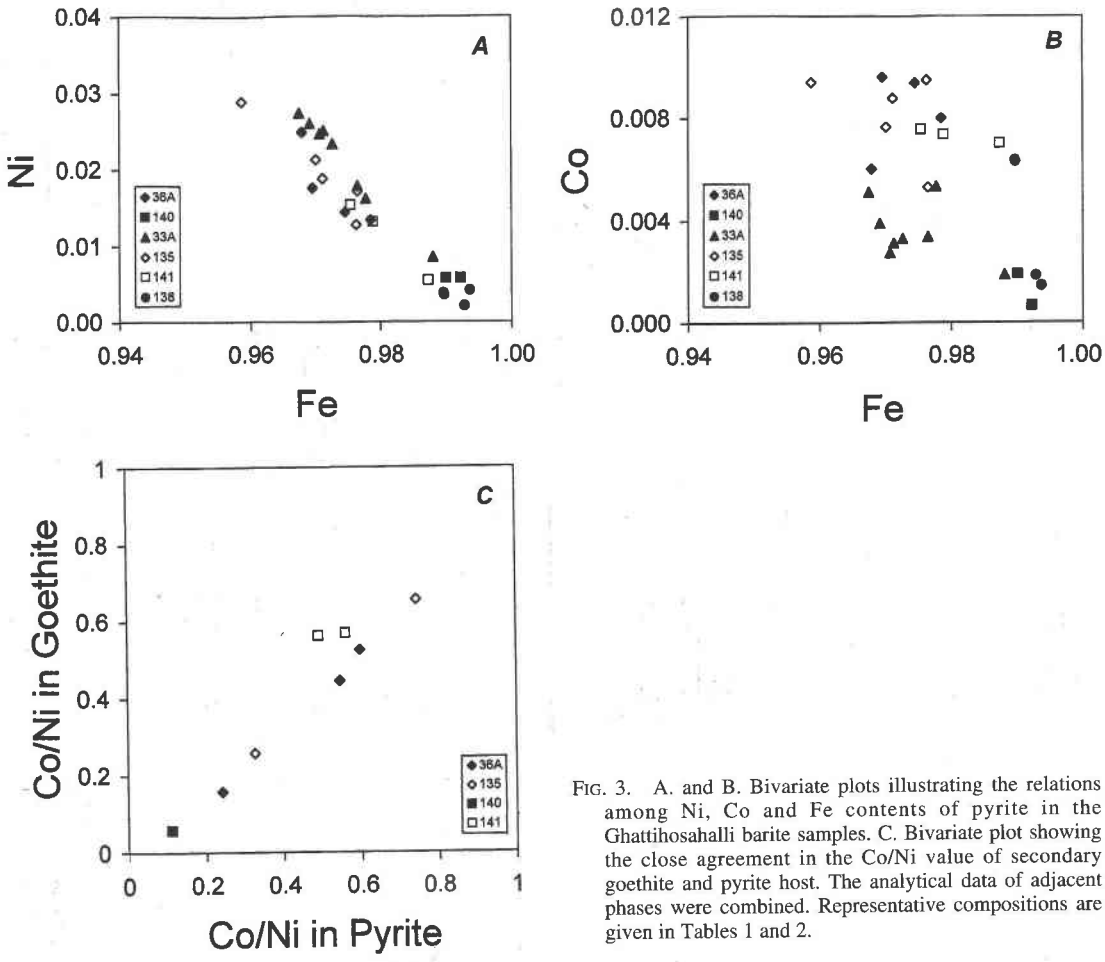

FIG. 3. A. and B. Bivariate plots illustrating the relations among Ni, Co and Fe contents of pyrite in the Ghattihosahalli barite samples. C. Bivariate plot showing the close agreement in the Co/Ni value of secondary goethite and pyrite host. The analytical data of adjacent phases were combined. Representative compositions are given in Tables 1 and 2.

The Cr amounts to 0.4–0.8 *apfu*; in one extreme case, the tourmaline contains 2.5 *apfu*, the highest reported so far (Table 6, Fig. 7B).

Chromian epidote is recorded only in the samples of fine-grained barite. It occurs in yellowish green anhedral to subhedral grains showing weak to moderate zoning. Like the other silicate minerals of the Ghattihosahalli suite, the epidote also is rich in Cr (Table 7). The compositions obtained for epidote grains present in two samples essentially correspond to ternary solid-solutions in the system zoisite – $[Fe^{3+}Al_2]$-epidote – $[Cr^{3+}Al_2]$-epidote ("tawmawite") (Fig. 8). There is a considerable solid-solution toward the chromian end-member, the rim compositions of zoned grains in sample 141 containing up to 80 mol.% of the chromian end-member. Notable concentrations of Ce and V are present (Table 7).

Chromian garnet was noted as emerald green anhedral to subhedral grains only in sample 141 of fine-grained barite. It is essentially a binary solid-solution between uvarovite and grossular ($Uva_{61}Grs_{34}$ – $Uva_{41}Grs_{52}$), with the components pyrope, almandine and spessartine making up less than 10 mol.% (Fig. 9, Table 8). The garnet also contains 0.04 to 0.09 *apfu* V^{3+} in the octahedral sites. Raase *et al.* (1983) have reported a more strongly chromiferous garnet ($Uva_{70}Grs_{28}$) from this locality, in a sample of chromian muscovite quartzite with layers of barite. The somewhat low analytical totals of the chromian garnet may be attributed to the presence of a minor hydrogarnet component.

Nearly euhedral tiny crystals of chromiferous *rutile* (0.7 to 2.8 wt.% Cr_2O_3) and *titanite* (1.2–1.6 wt.% Cr_2O_3) occur sporadically in the fine-grained and siliceous portions of barite (Table 9). Locally, rutile is altered to a hydrous secondary mineral with up to 7.1 wt.% Cr_2O_3, 3 wt.% V_2O_3, 3.3 wt.% Al_2O_3 and 4.2 wt.% SiO_2. *Graphite* occurs as soft, lead-gray flakes in rare patches and specks, particularly in the coarse-grained barite.

TABLE 3. REPRESENTATIVE COMPOSITIONS OF K,Ba-FELDSPAR AND ALBITE IN BARITE SEAMS FROM GHATTIHOSAHALLI

Sample	28		29	137	137B				135		29	28
Analysis	1#	2#	3#	4#	5#	6#	7#	8#	9#	10#	11#	12#
SiO_2 wt.%	61.54	62.64	60.57	52.57	44.83	47.09	41.62	39.70	33.62	38.79	65.79	67.88
Al_2O_3	18.92	19.09	19.18	21.68	23.24	22.77	23.93	24.60	25.18	24.91	20.55	19.94
CaO	0.00	0.00	0.00	0.02	0.01	0.00	0.00	0.00	0.04	0.01	1.24	0.20
Na_2O	0.42	0.34	0.56	0.85	1.04	1.19	0.78	0.59	0.27	0.41	11.75	12.03
K_2O	15.32	14.62	14.62	10.21	5.73	6.73	4.56	3.93	0.97	3.00	0.05	0.07
BaO	3.26	3.78	4.50	14.21	24.65	21.90	28.63	30.70	39.47	32.69	0.00	0.00
Total	99.50	100.50	99.43	99.54	99.62	99.70	99.58	99.61	99.62	99.81	99.41	100.15
Formulae based on 8 atoms of oxygen												
Si apfu	2.930	2.945	2.907	2.689	2.471	2.538	2.370	2.300	2.098	2.303	2.913	2.968
Al	1.062	1.058	1.085	1.307	1.510	1.446	1.606	1.680	1.852	1.743	1.073	1.028
Ca	0.000	0.000	0.000	0.001	0.001	0.000	0.000	0.000	0.003	0.001	0.059	0.008
Na	0.078	0.031	0.052	0.084	0.111	0.125	0.086	0.067	0.033	0.047	1.009	1.020
K	0.931	0.877	0.895	0.666	0.403	0.463	0.332	0.291	0.077	0.226	0.003	0.004
Ba	0.061	0.070	0.085	0.284	0.533	0.433	0.639	0.697	0.965	0.746	0.000	0.000
Molar proportions (%)												
Ab	3.8	3.2	5.0	8.1	9.3	4.7	12.1	6.7	7.3	4.6	94.2	98.7
Or	90.3	89.7	86.7	64.4	58.2	54.1	40.7	35.1	28.4	22.2	0.3	0.4
Cn	5.9	7.1	8.3	27.5	32.5	41.2	47.2	58.2	64.3	73.2	0.0	0.0
An	0.0	0.0	0.0	0.0	0.0	0.0	0.0	0.0	0.0	0.0	5.5	0.9

TABLE 3. (continued)

Sample	138									
Analysis	13#	14#	15#	16#	17#	18#	19#	20#	21#	22#
SiO_2 wt.%	62.96	62.14	51.08	48.64	46.92	43.45	41.47	38.79	36.00	33.11
Al_2O_3	18.19	18.95	22.02	22.13	22.73	23.79	24.21	24.91	25.85	26.54
CaO	0.00	0.02	0.01	0.00	0.00	0.00	0.01	0.01	0.00	0.02
Na_2O	0.06	0.46	0.95	0.46	1.18	0.62	0.67	0.41	0.36	0.17
K_2O	16.68	15.76	9.05	8.18	6.04	4.98	3.98	3.00	1.62	0.40
BaO	1.96	2.89	16.49	20.39	22.82	26.96	29.48	32.69	35.90	39.82
Total	99.85	100.22	99.61	99.80	99.79	99.80	99.83	99.81	99.73	100.06
Formulae based on 8 atoms of oxygen										
Si apfu	2.970	2.943	2.649	2.649	2.536	2.427	2.362	2.303	2.165	2.053
Al	1.011	1.055	1.345	1.391	1.448	1.565	1.625	1.743	1.832	1.940
Ca	0.000	0.001	0.001	0.000	0.000	0.000	0.000	0.001	0.000	0.001
Na	0.006	0.042	0.096	0.048	0.124	0.068	0.074	0.047	0.042	0.021
K	1.003	0.949	0.599	0.557	0.416	0.355	0.289	0.226	0.125	0.032
Ba	0.036	0.053	0.334	0.425	0.482	0.587	0.655	0.746	0.840	0.960
Molar proportions (%)										
Ab	0.6	4.0	9.3	4.7	12.1	6.7	7.3	4.6	4.2	2.0
Or	96.0	90.9	58.2	54.1	40.7	35.1	28.4	22.2	12.4	3.2
Cn	3.4	5.1	32.5	41.2	47.2	58.2	64.3	73.2	83.4	94.8
An	0.0	0.0	0.0	0.0	0.0	0.0	0.0	0.0	0.0	0.0

Discussion

Whereas several deposits of barite are known to occur in the Archean stratigraphic columns of southern Africa (Reimer 1980, 1990), reported occurrences of barite deposits of Archean age outside southern Africa are limited (*e.g.*, Pan & Fleet 1991). Archean barite deposits are generally described as forming bedded and stratiform deposits, and are interpreted as being essentially or partly sedimentary, volcanic-exhalative and placer deposits. Biological processes also have been proposed to explain the formation of these deposits (*cf.* Dunlop 1978).

In terms of the occurrence of a suite of Cr-enriched minerals and Ba-enriched feldspar, the layers of fine-grained barite at Ghattihosahalli bear considerable simi-

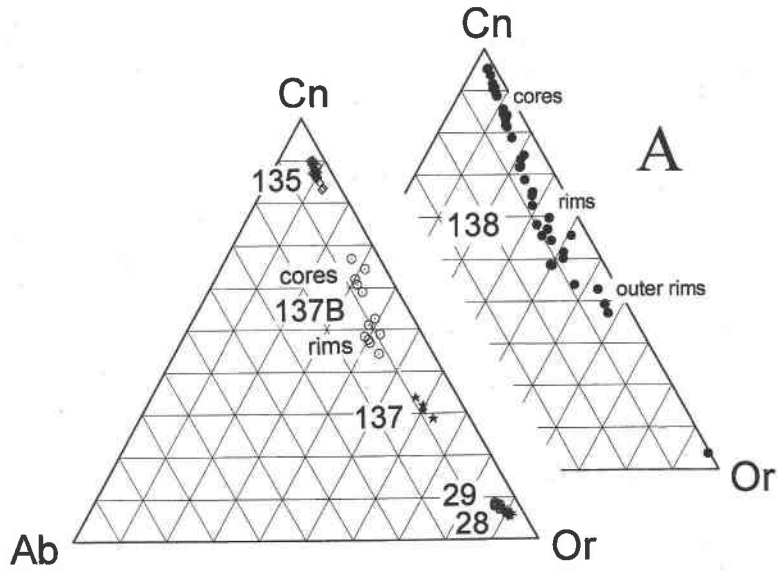

FIG. 4. A. Celsian (Cn)–K–feldspar (Or)–albite (Ab) diagrams showing the compositional variation of K,Ba-feldspar solid-solutions in several samples of barite from Ghattihosahalli. Representative compositions are given in Table 3. B. Line-scan illustrating the complex pattern of zoning in K,Ba-feldspar in barite sample 138. Note the distinct discontinuities with compositional gaps between Cn_{90}–Cn_{70} and Cn_{58}–Cn_{40}.

larity with the assemblages described from the Hemlo area, Ontario (Pan & Fleet 1991). The two are comparable in terms of age, both being Archean. They also resemble the assemblage described by Challis *et al.* (1995) from northwestern Nelson, New Zealand, and the Ba-enriched feldspar – muscovite association described by Chabu & Boulègue (1992) from the Kipushi Zn–Pb–Cu deposit, Shaba, Democratic Republic of Congo. Whereas the Hemlo assemblages represent predominantly chromiferous shaly sediments, those of Nelson and Shaba constitute quartzite – biotite schist – marble – carbonated ultramafic rock and dolomite – dolomitic shale associations, respectively. The barium-rich assemblage of Ghattihosahalli is distinctive and unique, however.

The occurrence of barite in the form of thin discontinuous seams interstratified with the quartzites, the similarity in textural and structural characteristics and metamorphic histories of the two rocks (Chadwick *et al.* 1985), and the presence of a similar suite of chromian and barian mineral phases in both the lithologies (this work, Raase *et al.* 1983) are all features indicative of a comparable genesis. Veins of barite are absent in the study area, and there is no obvious evidence of a genetic relation with the granitic intrusions to the west of the barite occurrence. The stratiform character points to a synsedimentary origin of both the barite seams and the associated quartzites. The fact that the barite seams are confined to a narrow stratigraphic zone of 5 to 20 m suggests that the basinal conditions favoring the deposition of barite lasted only for a short time. Further, the occurrence of the barite layers close to the underlying ultrabasic to basic metavolcanic rocks indicates deposition soon after their formation.

We envisage a volcanic–exhalative to sedimentary chemical deposition of the barite. An entirely chemogenic nature is likely for the relatively pure and coarse barite seams. For the impure fine-grained barite seams, apart from chemical precipitation, addition of a significant proportion of argillaceous material is indicated by the presence of Ba,Cr-bearing mica, tourmaline, epidote, garnet, rutile, and titanite. A similar interplay of chemical precipitation and clastic sedimentation has been advocated by Raase *et al.* (1983) for the closely associated chromiferous quartzites, mica schists and kyanite–mica schists. The sulfate–sulfide association, the significant chromium content, and the presence of Ni,Co-bearing pyrite are all features supportive of an interpretation of the Ghattihosahalli barite seams as submarine volcanic–exhalative. The Co/Ni values of the pyrite, 0.10 to 1.30, also indicate an early diagenetic to volcanic–exhalative formation (see Keith & Degens 1959, Pandalai *et al.* 1983, Howard & Hanor 1987). The chromium in the system originated through hydrothermal leaching of the underlying basic–ultrabasic volcanic rocks.

The thorough metamorphic recrystallization under conditions of the medium-amphibolite facies has completely modified the original mineralogy of the barite

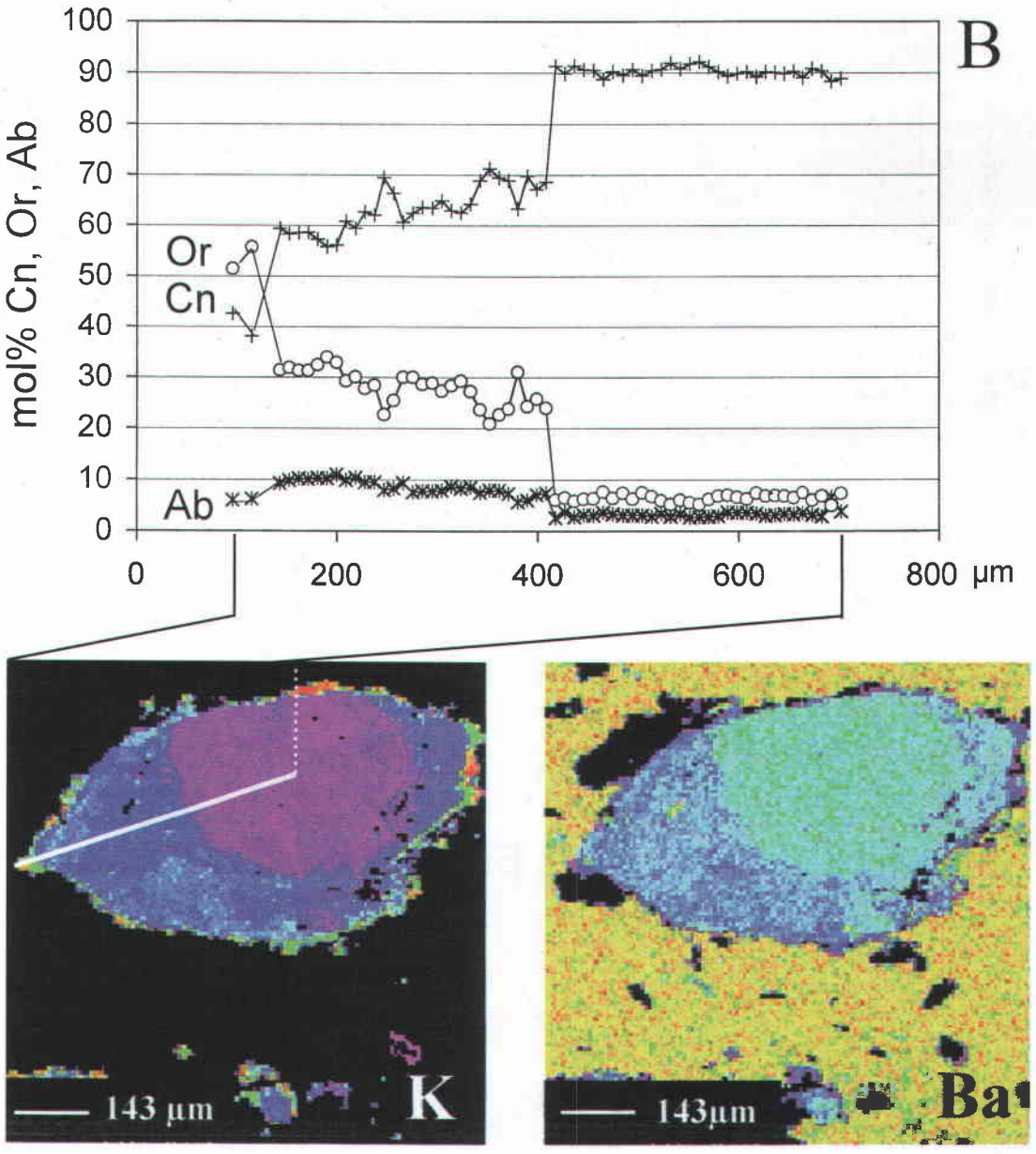

seams, and no definite inferences can be drawn regarding this aspect, as well as the prograde paragenetic evolution. It is possible that barite, quartz and K,Ba-feldspar already constituted penecontemporaneous chemical precipitates *i.e.*, authigenic phases. Alternatively, the celsian may have formed through dehydration of a cymrite-like precursor phase [$(BaAl_2Si_2)(O,OH)_8 \cdot H_2O$] (Chabu & Boulègue 1992) or by low-grade metamorphic reaction of barite with kaolinite. Similarly, the formation of intermediate K,Ba-feldspar compositions may also be attributed to prograde metamorphic reactions involving barite, clay minerals (kaolinite, illite), muscovite and quartz. The aqueous phase may also have supplied the potassium required in the reactions.

The considerable variations recorded in the compositions of the K,Ba-feldspar, the Ba–Cr mica and the other chromian mineral phases, from one seam to the other and even within the scale of individual micro-

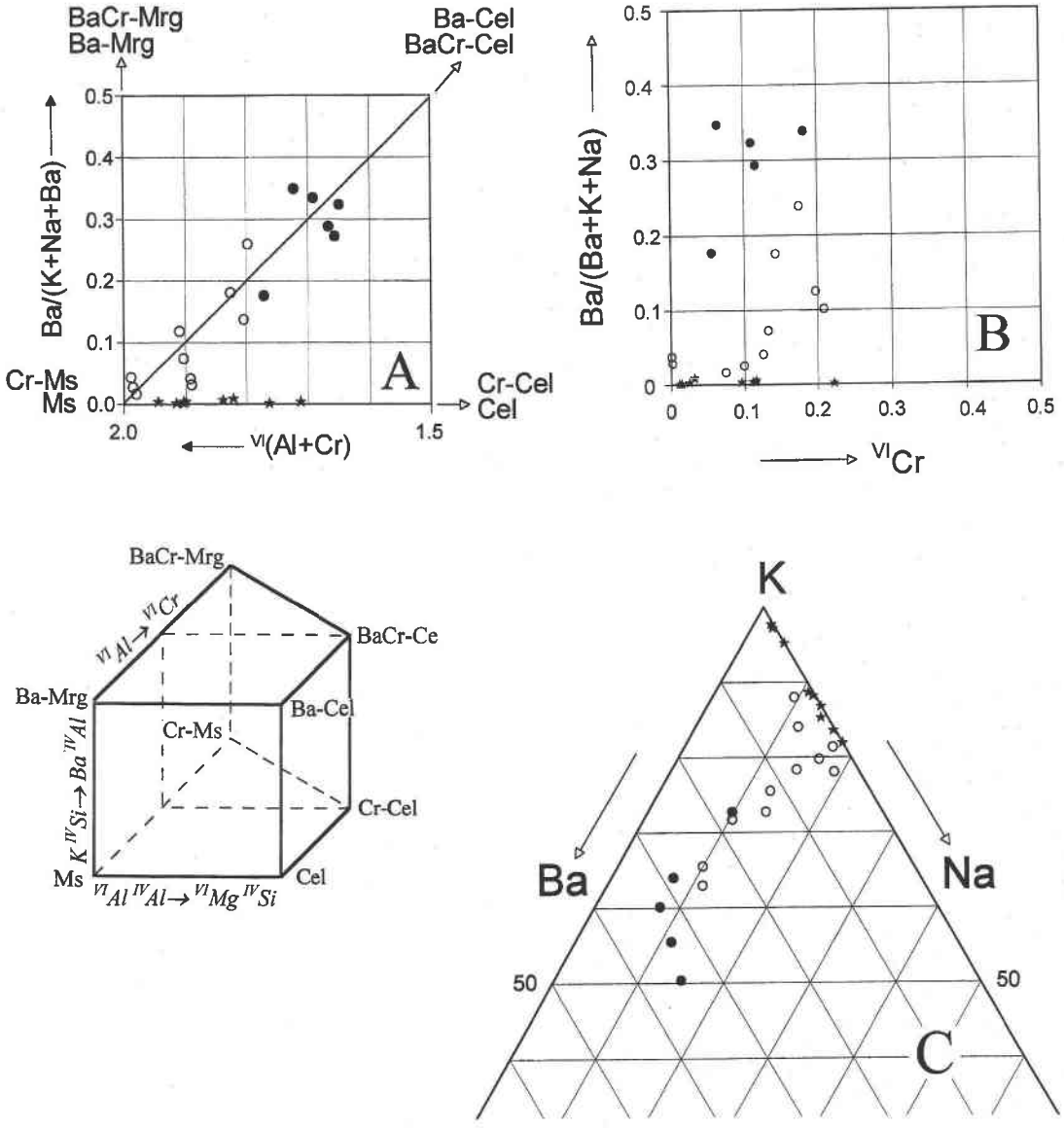

FIG. 5. Compositional variation of Ba,Cr-bearing mica in barite and chromiferous quartzite samples from Ghattihosahalli. A and B. Projections on two sides of the composition space defined by the end-members muscovite (Ms), celadonite (Cel), barium equivalent of margarite (Ba–Mrg), barium equivalent of celadonite (Ba–Cel) and their chromian analogues (after Raase *et al.* 1983). C. K–Na–Ba diagram showing the interlayer occupancy of the micas. Representative compositions are given in Table 4. Filled circles: mica in barite, open circles: mica in chromiferous quartzite samples, stars: chromian mica from Sargur-type quartzites that are not associated with barite (data from Raase *et al.* 1983).

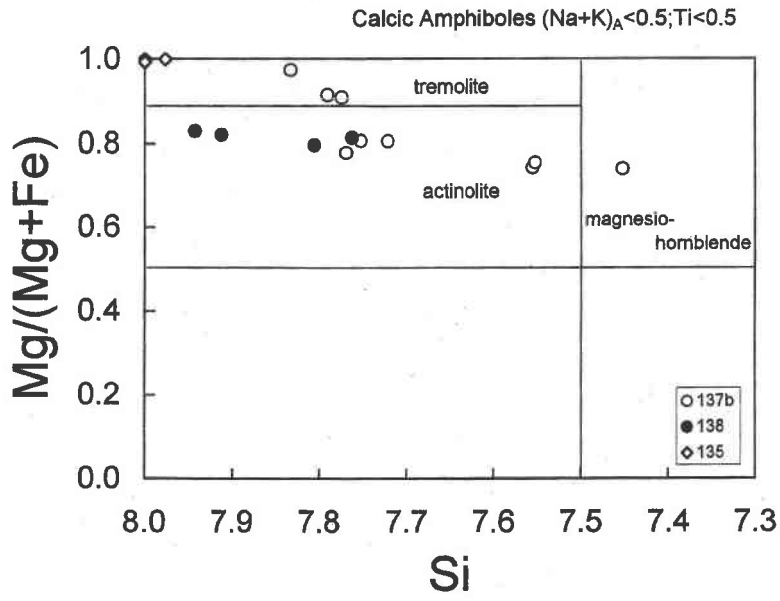

FIG. 6. Classification of amphiboles in barite seams from Ghattihosahalli in terms of Mg/(Mg + Fe) and Si. Representative compositions are given in Table 5.

TABLE 4. REPRESENTATIVE COMPOSITIONS OF Ba,Cr-BEARING MICA IN BARITE SEAMS FROM GHATTIHOSAHALLI

Sample	36A		137		32		33A		31A	
Analysis	#42	#44	#20	#24	#1	#4	#1	#13	#7	#14
SiO_2 wt.%	39.24	40.19	40.57	41.26	38.58	38.97	39.82	38.22	37.99	38.69
TiO_2	1.55	1.91	1.29	1.49	1.62	1.29	0.88	1.58	1.88	1.79
Al_2O_3	31.59	31.57	33.55	32.89	31.43	33.54	35.36	34.48	31.83	31.89
Cr_2O_3	2.24	1.94	0.98	1.18	3.13	0.88	0.48	0.89	2.20	1.67
FeO	0.81	0.66	1.60	1.14	0.36	0.50	0.05	0.13	0.50	0.90
MnO	0.00	0.00	0.01	0.00	0.00	0.00	0.00	0.00	0.00	0.00
MgO	1.67	1.68	0.68	0.81	1.69	1.30	1.15	0.94	1.53	1.66
CaO	0.00	0.03	0.04	0.00	0.01	0.00	0.01	0.01	0.02	0.00
BaO	9.64	11.51	6.26	5.91	11.80	11.01	12.90	12.77	11.66	11.40
Na_2O	0.65	0.55	0.71	0.87	0.80	0.66	1.25	0.99	0.60	0.39
K_2O	7.37	6.57	7.96	7.94	6.02	6.47	4.94	4.95	6.55	6.84
Total	94.76	96.61	93.65	93.49	95.44	94.62	96.84	94.96	94.76	95.23
Formulae based on 11 atoms of oxygen										
Si apfu	2.847	2.877	2.895	2.934	2.812	2.827	2.822	2.776	2.791	2.821
^{IV}Al	1.153	1.123	1.105	1.066	1.188	1.173	1.178	1.224	1.209	1.179
^{VI}Al	1.549	1.510	1.716	1.690	1.511	1.714	1.775	1.727	1.547	1.561
Ti	0.085	0.103	0.069	0.800	0.089	0.070	0.047	0.086	0.104	0.098
Cr	0.129	0.110	0.055	0.066	0.180	0.050	0.027	0.051	0.128	0.096
Fe	0.049	0.040	0.095	0.068	0.022	0.030	0.003	0.008	0.031	0.055
Mn	0.000	0.000	0.001	0.000	0.000	0.000	0.000	0.000	0.000	0.000
Mg	0.181	0.179	0.072	0.086	0.184	0.141	0.121	0.102	0.168	0.180
Ca	0.000	0.002	0.003	0.000	0.001	0.000	0.001	0.001	0.002	0.000
Ba	0.274	0.323	0.175	0.165	0.337	0.313	0.358	0.363	0.336	0.326
Na	0.091	0.076	0.098	0.120	0.113	0.093	0.172	0.139	0.085	0.055
K	0.682	0.600	0.724	0.720	0.560	0.599	0.447	0.459	0.614	0.636

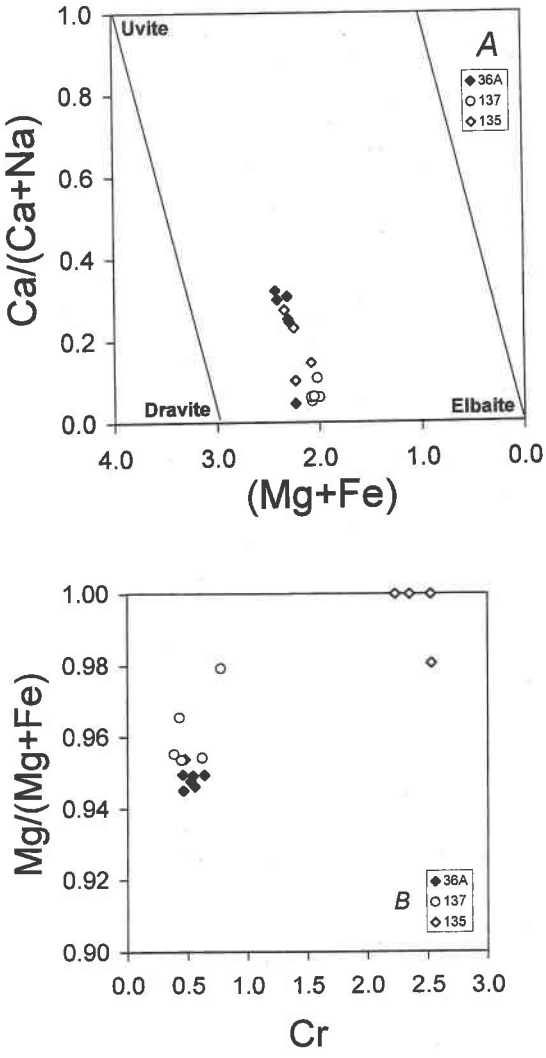

FIG. 7. Ca/(Ca + Na) *versus* (Mg + Fe) and Mg/(Mg + Fe) *versus* Cr plots illustrating the compositional variation of tourmaline in barite seams from Ghattihosahalli. Representative compositions are given in Table 6.

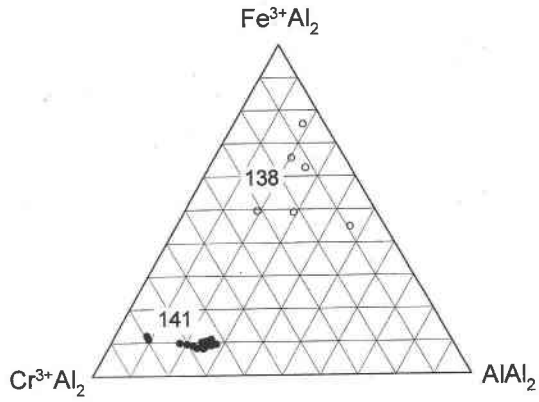

FIG. 8. Compositional variation of epidote in barite seams from Ghattihosahalli, in terms of the end-members zoisite [$Ca_2AlAl_2Si_3O_{12}(OH)$], epidote [$Ca_2Fe^{3+}Al_2Si_3O_{12}(OH)$] and the chromian end-member [$Ca_2Cr^{3+}Al_2Si_3O_{12}(OH)$]. Representative compositions are given in Table 7.

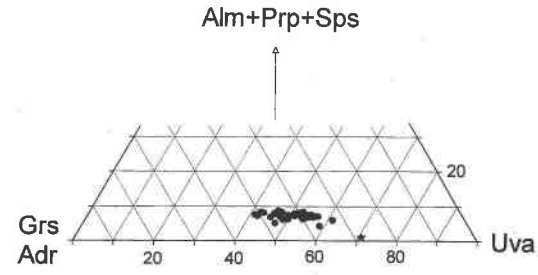

FIG. 9. (Grs + Adr) – Uva – (Alm + Prp + Sps) diagram showing the compositional variation of chromian garnet in barite seams from Ghattihosahalli. Filled circles: sample 138 (this study); star: sample 163 VIII (Raase *et al.* 1983).

bands, reflect the chemical inhomogeneity in the precursor sediment. Apparently, the element migration (Cr, Ba) during medium-grade metamorphism was so limited that it did not lead to small-scale chemical homogenization (*cf.* Sánchez-Vizcaíno *et al.* 1995). However, the rather well-defined patterns of Cr partitioning for the coexisting phases mica, tourmaline, rutile and spinel in chromiferous banded quartzites from the same Archean domain, reported by Raase *et al.* (1983), indicate attainment of chemical equilibrium among the mineral phases on the scale of a thin section.

ACKNOWLEDGEMENTS

This work was carried out at the Institute for Mineralogy and Petrology, University of Bonn, during the tenure of a DAAD fellowship held by the first author. We express our sincere thanks to B.K. Wodeyar and G. Subbarao for their assistance during field work. R.A. Howie, F.G.B. Poole, T.K. Lowenstein and B.P. Radhakrishnan provided constructive comments on an early version of the manuscript. The paper has benefitted from reviews by J.B. Maynard and C. Ravenhurst. We thank R.F. Martin for his helpful suggestions and annotations.

TABLE 5. REPRESENTATIVE COMPOSITIONS OF CALCIC AMPHIBOLE IN BARITE SEAMS FROM GHATTIHOSAHALLI

Sample	137b				138		135
Analysis	#27	#28	#22	#17	#36	#42	#18
SiO_2 wt.%	56.69	55.67	54.28	51.35	56.15	54.71	58.91
TiO_2	0.00	0.04	0.00	0.14	0.00	0.06	0.00
Al_2O_3	1.75	2.12	2.28	4.36	1.00	2.48	0.52
Cr_2O_3	0.04	0.30	0.04	1.09	0.16	0.08	0.02
FeO	1.09	3.49	7.93	10.12	7.40	7.52	0.01
MnO	0.23	0.37	0.36	0.41	0.34	0.38	0.03
MgO	22.90	21.02	18.47	16.06	18.95	18.31	24.51
BaO	0.01	0.06	0.08	0.08	0.00	0.04	0.01
CaO	13.50	12.98	12.61	12.14	13.17	12.91	13.48
K_2O	0.04	0.08	0.04	0.13	0.02	0.09	0.02
Na_2O	0.20	0.31	0.37	0.73	0.12	0.31	0.07
Total	96.45	96.44	96.46	96.61	97.31	96.89	97.58
Formulae based on 23 atoms of oxygen							
Si apfu	7.833	7.791	7.753	7.452	7.912	7.763	7.977
^{IV}Al	0.167	0.209	0.247	0.548	0.088	0.237	0.023
^{VI}Al	0.118	0.141	0.137	0.194	0.078	0.178	0.060
Ti	0.000	0.004	0.000	0.015	0.000	0.006	0.000
Cr	0.004	0.033	0.005	0.125	0.018	0.009	0.002
Fe^{2+}	0.126	0.408	0.947	1.228	0.872	0.892	0.001
Mn	0.027	0.044	0.044	0.050	0.041	0.046	0.003
Mg	4.717	4.385	3.933	3.475	3.981	3.873	4.948
Ba	0.001	0.003	0.004	0.005	0.000	0.002	0.001
Ca	1.998	1.946	1.930	1.887	1.988	1.962	1.955
Na	0.054	0.084	0.102	0.205	0.033	0.085	0.018
K	0.008	0.014	0.007	0.024	0.004	0.016	0.003
Mg/(Mg+Fe)	0.974	0.915	0.806	0.739	0.820	0.813	1.000

TABLE 6. REPRESENTATIVE COMPOSITIONS OF Cr-BEARING TOURMALINE IN BARITE SEAMS FROM GHATTIHOSAHALLI

Sample	36A			137		135	
Analysis	#1	#6	#41	#16	#23	#24	#15
SiO_2 wt.%	37.05	36.07	36.30	36.56	36.37	35.20	35.01
TiO_2	0.10	0.28	0.32	0.21	0.02	0.04	0.08
Al_2O_3	31.91	31.49	31.50	33.73	31.73	19.01	20.95
Cr_2O_3	4.10	4.36	3.74	3.04	6.05	18.61	16.61
FeO	0.87	0.91	0.83	0.69	0.31	0.30	0.00
MnO	0.11	0.04	0.04	0.06	0.12	0.00	0.04
MgO	8.81	8.96	9.60	8.25	8.21	8.55	9.23
CaO	0.20	1.13	1.48	0.23	0.49	0.55	1.36
BaO	0.12	0.06	0.04	0.06	0.04	0.26	0.19
Na_2O	2.31	1.92	1.73	2.34	2.23	2.68	1.99
K_2O	0.00	0.04	0.02	0.03	0.01	0.04	0.07
Total	85.58	85.26	85.60	85.20	85.58	85.24	85.53
Formulae on the basis of 49 cation valences							
Si apfu	5.973	5.865	5.869	5.887	5.888	6.054	5.949
Ti	0.012	0.034	0.039	0.025	0.002	0.005	0.010
Al	6.062	6.034	6.002	6.401	6.053	3.853	4.196
Cr	0.523	0.560	0.478	0.387	0.774	2.531	2.232
Fe	0.117	0.124	0.112	0.093	0.042	0.043	0.000
Mn	0.015	0.006	0.005	0.008	0.016	0.000	0.006
Mg	2.117	2.172	2.314	1.980	1.981	2.192	2.338
Ba	0.008	0.004	0.003	0.004	0.003	0.018	0.013
Ca	0.035	0.197	0.256	0.040	0.085	0.101	0.248
Na	0.722	0.605	0.542	0.730	0.700	0.894	0.656
K	0.000	0.008	0.004	0.006	0.002	0.009	0.015

TABLE 7. REPRESENTATIVE COMPOSITIONS OF EPIDOTE IN BARITE SEAMS FROM GHATTIHOSAHALLI

Sample	141				138			
Analysis	#40	#2	#27	#6	#52	#3	#10	#28
SiO_2 wt.%	37.45	37.54	37.10	37.41	37.94	38.20	38.03	37.33
TiO_2	0.13	0.19	0.12	0.08	0.10	0.09	0.09	0.02
Al_2O_3	21.61	21.85	23.70	23.62	22.53	23.73	22.72	22.00
Cr_2O_3	11.85	11.56	10.00	9.51	4.67	3.30	2.18	0.90
V_2O_3	nd	0.77	nd	0.30	nd	nd	nd	nd
Fe_2O_3	1.87	1.67	1.52	1.68	7.75	7.75	10.59	11.95
Mn_2O_3	0.20	0.20	0.24	0.20	0.22	0.22	0.32	0.38
MgO	0.23	0.17	0.11	0.12	0.04	0.06	0.03	0.01
CaO	22.11	22.04	22.70	23.03	22.67	22.99	23.07	22.97
Ce_2O_3	nd	nd	nd	0.11	nd	nd	nd	nd
Total	95.45	95.99	95.49	96.06	95.92	96.34	97.03	95.56
Formulae based on 25 atoms of oxygen								
Si apfu	6.095	6.076	6.006	6.024	6.132	6.120	6.103	6.102
Ti	0.016	0.023	0.015	0.010	0.012	0.011	0.011	0.002
Al	4.145	4.168	4.522	4.482	4.291	4.480	4.297	4.238
Cr	1.525	1.479	1.280	1.211	0.597	0.418	0.277	0.116
V	---	0.100	---	0.039	---	---	---	---
Fe^{3+}	0.229	0.203	0.185	0.203	0.943	0.935	1.278	1.470
Mn^{3+}	0.006	0.012	0.015	0.012	0.025	0.020	0.019	0.024
Mg	0.056	0.041	0.027	0.029	0.010	0.014	0.007	0.002
Ca	3.855	3.822	3.937	3.973	3.925	3.946	3.966	4.022
Ce	---	---	---	0.006	---	---	---	---

TABLE 8. REPRESENTATIVE COMPOSITIONS OF UVAROVITIC GARNET IN BARITE SEAMS FROM GHATTIHOSAHALLI

Sample	141				
Analysis	#9	#8	#12	#10	#11
SiO_2 wt.%	36.48	36.76	37.06	36.77	37.10
TiO_2	0.24	0.28	0.30	0.42	1.20
Al_2O_3	7.23	9.34	9.27	9.40	10.52
Cr_2O_3	17.97	15.88	15.27	14.68	13.05
V_2O_3	0.93	0.61	0.91	1.43	0.79
Fe_2O_3	1.51	0.35	1.11	1.41	0.56
FeO	0.01	1.02	0.68	0.31	1.14
MnO	1.30	1.38	1.25	0.91	1.17
MgO	0.26	0.41	0.41	0.53	0.59
CaO	32.39	31.83	32.56	32.58	32.43
Total	98.32	97.86	98.82	98.44	98.55
Formulae based on 24 atoms of oxygen					
Si apfu	5.978	5.995	5.988	5.953	5.966
Ti	0.030	0.034	0.036	0.051	0.145
Al	1.396	1.795	1.765	1.794	1.994
Cr	2.328	2.048	1.951	1.879	1.659
V	0.122	0.080	0.118	0.186	0.102
Fe^{3+}	0.279	0.064	0.202	0.258	0.102
Fe^{2+}	0.001	0.139	0.092	0.042	0.153
Mn	0.180	0.191	0.171	0.125	0.159
Mg	0.064	0.100	0.099	0.128	0.141
Ca	5.686	5.562	5.636	5.651	5.587
Molar proportions (%)					
Alm	0.0	2.3	1.5	0.7	2.5
Prp	1.1	1.7	1.6	2.2	2.3
Sps	3.0	3.2	2.9	2.1	2.6
Grs	29.9	40.0	40.1	41.1	48.8
Adr	7.1	1.6	5.1	6.5	2.5
Uva	58.9	51.3	48.8	47.4	41.2

TABLE 9. REPRESENTATIVE COMPOSITIONS OF RUTILE AND TITANITE IN BARITE SEAMS FROM GHATTIHOSAHALLI

	Rutile				Titanite	
Sample	32A		137		135	138
Point	#1	#2	#3	#4	#5	#6
SiO_2 wt.%	0.10	0.15	0.00	0.00	29.88	30.36
TiO_2	97.05	96.73	98.75	99.04	35.74	35.62
Al_2O_3	0.00	0.00	0.00	0.00	1.14	1.72
Cr_2O_3	2.01	2.23	0.69	0.87	1.58	1.20
V_2O_3	0.45	0.34	0.59	0.26	0.00	0.00
FeO	0.00	0.04	0.17	0.23	0.00	0.00
MnO	0.00	0.01	0.02	0.06	0.02	0.00
MgO	0.00	0.00	0.00	0.00	0.06	0.01
CaO	nd	nd	nd	nd	27.33	28.12
Total	99.61	99.50	100.22	100.46	95.75	97.03
Formulae based on 2 atoms of oxygen (rutile) and 4 atoms of Si (titanite)						
Si apfu	0.001	0.002	0.000	0.000	4.000	4.000
Ti	0.979	0.977	0.988	0.989	3.599	3.530
Al	0.000	0.000	0.000	0.000	0.180	0.267
Cr	0.021	0.024	0.007	0.009	0.167	0.062
V	0.005	0.004	0.006	0.003		
Fe	0.000	0.000	0.002	0.003	0.000	0.000
Mn	0.000	0.000	0.000	0.001	0.007	0.001
Mg	0.000	0.000	0.000	0.000	0.004	0.000
Ca					3.920	3.969

References

ANNAIYA, G.S. & SRINIVASAIAH, C. (1976): Barite deposit of Ghattihosahalli, Kumminaghatta, Janakal area, Holalkere and Hosadurga taluks, Chitradurga District. *Dep. Mines and Geol., Bangalore, Geol. Studies* **112**, 1-19

CHABU, M. & BOULÈGUE, L. (1992): Barian feldspar and muscovite from the Kipushi Zn–Pb–Cu deposit, Shaba, Zaire. *Can. Mineral.* **30**, 1143-1152.

CHADWICK, B., RAMAKRISHNAN, M. & VISWANATHA, M.N. (1981): Structural and metamorphic relations between Sargur and Dharwar supracrustal rocks and Peninsular gneiss in central Karnataka. *J. Geol. Soc. India* **22**, 557-569.

_____, _____ & _____ (1985): A comparative study of tectonic fabrics and deformation mechanisms in Dharwar grits and phyllites and Sargur quartzites of the west of the Chitradurga Supracrustal belt, Karnataka. *J. Geol. Soc. India* **26**, 526-546.

_____, _____, _____ & SRINIVASA MURTHY, V. (1978): Structural studies in the Archean Sargur and Dharwar supracrustal rocks of the Karnataka Craton. *J. Geol. Soc. India* **19**, 531-549.

CHALLIS, A., GRAPES, R. & PALMER, K. (1995): Chromian muscovite, uvarovite and zincian chromite: products of regional metasomatism in northwest Nelson, New Zealand. *Can. Mineral.* **33**, 1263- 1284.

DEVARAJU, T.C. & ANANTHA MURTHY, K.S. (1978): Mineralogy of the fuchsites from Ghattihosahalli, Chitradurga District. *Proc. Indian Acad. Sci.* **87A**, 255-261.

_____ & _____ (1979): Optical and X-ray study and genesis of barytes from Ghattihosahalli, Chitradurga district. *J. Geol. Soc. India* **20**, 501-506.

_____ & RAITH, M. (1990): A sedimentary barite deposit in an early Archean greenstone belt of Karnataka, India. *8th IAGOD Symp. (Ottawa), Abstr. Vol.*, A6.

DUNLOP, J.S. (1978): Shallow water sedimentation of North Pole, Pilbara Block, Western Australia. *In* Archean Cherty Metasediments: their Sedimentology, Micropalaeontology, Biogeochemistry and Significance to Mineralisation (T.E. Glover & D.I. Groves, eds.). *Publ. Geol. Dep., Univ. Western Australia* **2**, 30-88.

HOERING, T.C. (1989): The isotopic composition of bedded barite from the Archean southern India. *J. Geol. Soc. India* **34**, 38-61.

HOWARD, K.W. & HANOR, J.S. (1987): Composition and zoning in the Fancy Hill stratiform barite deposit, Ouachita Mountains, Arkansas, and evidence for the lack of associated massive sulfides. *Econ. Geol.* **82**, 1377-1385.

KEITH, M.C. & DEGENS, E.S. (1959): Geochemical indications of marine and fresh-water sediments. *In* Researches in Geochemistry **1** (P.H. Abelson, ed.). John Wiley & Sons, New York, N.Y. (38-61).

NAQVI, S.M. (1978): Geochemistry of Archean metasediments: evidence for prominent anorthosite – norite – troctolite (ANT) in the Archean basaltic primordial crust. *In* Archean Geochemistry (B.F. Windley & S.M. Naqvi, eds.). Elsevier, Amsterdam, The Netherlands (343-360).

NARAYANA, B.L. & NAQVI, S.M. (1980): Geochemistry of spinifex-textured peridotitic komatiites from Ghatti Hosahalli, Karnataka, India. *J. Geol. Soc. India* **21**, 194-198.

PAN, YUANMING & FLEET, M.E. (1991): Barian feldspar, barian–chromian muscovite from the Hemlo area, Ontario. *Can. Mineral.* **29**, 481-498.

PANDALAI, H.S., MAJUMDER, T. & CHANDRA, D. (1983): Geochemistry of pyrite and black shales of Amjhore, Rohtas District, Bihar, India. *Econ. Geol* **78**, 1505-1513.

POUCHOU, J.-L. & PICHOIR, F. (1984): A new model for quantitative X-ray microanalysis. I. Application to the analysis of homogeneous samples. *La Recherche Aérospatiale* **3**, 167-192.

RAASE, P., RAITH, M., ACKERMAND, D., VISWANATHA, M.N. & LAL, R.K. (1983): Mineralogy of chromiferous quartzites from South India. *J. Geol. Soc. India* **24**, 502-521.

RADHAKRISHNA, B.P. & SREENIVASAIYA, C. (1974): Bedded barytes from the Precambrian of Karnataka. *J. Geol. Soc. India* **15**, 314-317.

REIMER, T.O. (1980): Archean sedimentary barite deposits of Swaziland Supergroup (Barberton Mountain Land, South Africa). *Precambrian Res.* **12**, 393-410.

_____ (1990): Archean barite deposits of southern Africa. *J. Geol. Soc. India* **35**, 131-150.

SÁNCHEZ-VIZCAÍNO, V.L., FRANZ, G. & GÓMEZ-PUGNAIRE, M.T. (1995): The behavior of Cr during metamorphism of carbonate rocks from the Nevado–Filabride Complex, Betic Cordilleras, Spain. *Can. Mineral.* **33**, 85-104.

SESHADRI, T.S., CHAUDHURI, A., HARINADHA BABU, P. & CHAYAPATHI, N. (1981): Chitradurga Belt. *In* Early Precambrian Supracrustals of Southern Karnataka (J. Swami-Nath & M. Ramakrishnan, eds). *Geol. Surv. India, Mem.* **112**, 163-198.

TAYLOR, P.N., CHADWICK, B., MOORBATH, S., RAMAKRISHNAN, M. & VISWANATHA, M.N. (1984): Petrography, chemistry and isotopic ages of Peninsular Gneiss, Dharwar acid volcanic rocks and the Chitradurga granite with special reference to the late Archean evolution of the Karnataka craton, southern India. *Precambrian Res.* **23**, 349-375.

TRACY, R.J. (1991): Ba-rich micas from the Franklin Marble, Lime Crest and Sterling Hill, New Jersey. *Am. Mineral.* **76**, 1683-1693.

VISWANATHA, M.N., RAMAKRISHNAN, M. & NARAYANAN KUTTY, T.R. (1977): Possible spinifex texture in a serpentinite from Karnataka. *J. Geol. Soc. India* **18**, 194-197.

Received September 22, 1998, revised manuscript accepted February 17, 1999.